

Dynamical gap from holography in the charged dilaton black hole

Xiao-Mei Kuang¹, Bin Wang¹, and Jian-Pin Wu^{2,3,4}

¹*INPAC, Department of Physics and Shanghai Key Lab for Particle Physics and Cosmology,
Shanghai Jiao Tong University, Shanghai 200240, China*

²*Department of Physics, Hanyang University, Seoul 133-791, Korea*

³*Center for Quantum Spacetime, Sogang University, Seoul 121-742, Korea*

⁴*Department of Physics, School of Mathematics and Physics, Bohai University, JinZhou, 121013, China*

Abstract

We study the holographic non-relativistic fermions in the presence of bulk dipole coupling in charged dilatonic black hole background. We investigate the nontrivial effects of the bulk dipole coupling, the dilaton field and the charge on the non-relativistic fermion system. We find that the dual boundary theory exhibits a number of interesting properties with the change of these parameters.

PACS numbers: 11.25.Tq, 04.50.Gh, 71.10.-w

I. INTRODUCTION

The AdS/CFT correspondence is a powerful method to investigate the strongly coupled many body phenomena by relating certain interacting quantum field theories to classical gravity systems. An interesting application of such duality is the study of condensed matter physics from the remarkable connection in gravitational physics, for reviews see for examples [1–3].

Stimulated by the AdS/CFT correspondence, the simplest realization to construct gravitational duals of the transition from normal state to superconducting state is to deal with Einstein’s gravitational theory with a negative cosmological constant coupled to a gauge field. While this idea caught some interesting properties of the realistic superconductor, the classical example using the simplest charged AdS black hole as gravitational background is not physical in the low temperature limit, since it contains nonzero entropy even at zero temperature. Such gravitational configuration cannot be employed to explain the Fermi liquid behavior on its boundary condensed matter system in which the entropy should be linearly dependent of the temperature. This situation was improved by changing the background bulk geometry to include a real scalar field, the dilaton, which allows zero entropy at zero temperature [4–6].

In addition to modifying the bulk gravitational backgrounds, recently there have been some attempts to modify the boundary conditions in describing the condensed matter system. In [7], it was shown that one can implement the holographic non-relativistic fermionic fixed points by imposing Lorentz breaking boundary conditions instead of the Lorentz covariant one on the Dirac spinor field, which can lead to the presence of an infinite flat band in the boundary field theory. Further studies on the holographic non-relativistic fermionic fixed points have been reported in [8, 9]. In [10, 11], the holographic non-relativistic fermionic fixed points were studied in the charged dilatonic black hole and black brane.

To capture more general features and phenomena relating to condensed matter physics, there have been a lot of investigations to consider a quantum field theory which contains fermions charged under a global $U(1)$ symmetry [12–18]. However, many of these studies concentrated on the fermions minimally coupled to gravity and gauge fields. Recently, introducing the coupling between the fermion and gauge field through a dipole interaction in the bulk charged AdS black hole background, it was remarkably found that as the strength of the interaction is varied, spectral density is transferred and beyond the critical interaction strength a gap opens up[19]. The existence of Fermi surfaces as the varying of the dipole coupling was also disclosed[20]. The

extensions of the investigation on the dipole coupling to different bulk backgrounds were reported in [21–23].

In this work we will extend the study of the dipole interaction to the charged dilatonic AdS black hole background. Considering that different from the charged AdS black hole, the charged dilatonic AdS black hole has vanishing entropy in the low temperature limit, it is a suitable bulk background to study the holographic Fermi liquid. Furthermore, the dilaton can couple directly not only to the gauge field but also to the charged scalar, which can help to further disclose the role played by the dipole coupling in the boundary theory of Fermi liquid. In our study, instead of keeping Lorentz invariance for the boundary theory, we will impose Lorentz violating boundary terms for a spinor field following [7]. We will investigate the holographic spectral function behaviors at the non-relativistic fermionic fixed points and compare with the situations at the relativistic fermionic fixed point[22]. We will disclose how the effects of dilaton and the dipole coupling modify the properties of Fermi gap, Fermi momentum etc. in the Fermi system.

The organization of this paper is as follows. In section II, we will derive the bulk Dirac equations in 4-dimensional charged dilatonic AdS black hole. Then we will briefly discuss the holographic calculations of the retarded Green functions of those fermionic operators for non-relativistic theory. In section III, we will present our numerical results for the non-relativistic fixed point in different cases. Finally in section IV, we will summarize our results.

II. HOLOGRAPHIC SETUP

In this section, we will derive the Dirac equations of the bulk fermion coupling to the gauge field through dipole interaction in the charged dilatonic AdS black hole background. We will employ the Lorentz violating boundary term for the spinor field and study the holographic fermionic systems through the perturbations on the non-relativistic fermionic fixed point.

A. Dirac equation

We consider the non-minimal coupling between a spin-1/2 fermions and the gauge field in the form of the dipole interaction described by the bulk action

$$S_{bulk} = i \int d^d x \sqrt{-g} \zeta \left(\Gamma^a \mathcal{D}_a - m - ip \not{F} \right) \zeta, \quad (1)$$

where m and p are the mass of the fermion field and the dipole coupling parameter, respectively. In the action, $\Gamma^a = (e_\mu)^a \Gamma^\mu$, $\not{F} = \frac{1}{4} \Gamma^{\mu\nu} (e_\mu)^a (e_\nu)^b F_{ab}$ and $\mathcal{D}_a = \partial_a + \frac{1}{4} (\omega_{\mu\nu})_a \Gamma^{\mu\nu} - iq A_a$, with $\Gamma^{\mu\nu} = \frac{1}{2} [\Gamma^\mu, \Gamma^\nu]$ and the spin

connection $(\omega_{\mu\nu})_a = (e_\mu)^b \nabla_a (e_\nu)_b$, where $(e_\mu)^a$ forms a set of orthogonal normal vector bases[24].

We intend to work in the charged dilatonic AdS black hole background with the metric

$$ds^2 = -g_{tt}dt^2 + g_{xx}(d\vec{x})^2 + g_{rr}dr^2 = e^{2B}[-f dt^2 + (d\vec{x})^2] + \frac{1}{e^{2B}} \frac{dr^2}{f}, \quad F = dA, \quad \phi = \frac{1}{2} \ln(1 + \frac{Q}{r}),$$

$$B = \ln \frac{r}{L} + \frac{3}{4} \ln(1 + \frac{Q}{r}), \quad f = 1 - \frac{\nu L^2}{(Q+r)^3}, \quad A_a = (\frac{\sqrt{3Q\nu}}{Q+r} - \frac{\sqrt{3Q\nu}^{\frac{1}{6}}}{L^{\frac{2}{3}}})(dt)_a, \quad (2)$$

which is a solution to the Einstein-Maxwell-Dilaton action in 4-dimensional spacetime[4]

$$S_g = \frac{1}{16\pi G} \int_M d^4x \sqrt{-g} [R - \frac{1}{4} e^\phi F_{ab} F^{ab} - \frac{3}{2} \nabla_a \phi \nabla^a \phi + \frac{6}{L^2} \cosh \phi]. \quad (3)$$

Here, R and L are the Ricci scalar and the AdS radius, respectively. ϕ denotes the dilaton field and $F = dA$ is the field strength of $U(1)$ gauge field. The temperature of the charged dilaton black hole and chemical potential near the boundary read

$$T = \frac{g'_{tt}|_{r=r_+}}{4\pi} = \frac{3\nu^{\frac{1}{6}}}{4\pi L^{\frac{5}{3}}} \sqrt{r_+}, \quad \mu = -\frac{\sqrt{3Q\nu}^{\frac{1}{6}}}{L^{\frac{2}{3}}}, \quad (4)$$

where r_+ is the black hole horizon with the form $r_+ = \nu^{\frac{1}{3}} L^{\frac{2}{3}} - Q$ obtained from $f(r_+) = 0$. When $\nu = \frac{Q^3}{L^2}$, the black hole has zero temperature.

The Dirac equation $(\mathcal{D} - m - ip\not{F})\zeta = 0$ in the bulk has the form

$$(\sqrt{g^{rr}}\Gamma^r\partial_r - m - \frac{ip}{2}\sqrt{g^{rr}g^{tt}}\Gamma^{rt}\partial_r A_t)F - i(\omega + qA_t)\sqrt{g^{tt}}\Gamma^t F + ik\sqrt{g^{xx}}\Gamma^x F = 0, \quad (5)$$

after taking the ansatz $\zeta = (-g^{rr})^{-\frac{1}{4}} F e^{-i\omega t + ik_i x^i}$ and setting $k_i = k\delta_1^i$ without loss of generality. It is convenient to express F into $F = (F_1, F_2)^T$ and choose the following basis for our gamma matrices[25]

$$\Gamma^r = \begin{pmatrix} -\sigma^3 & 0 \\ 0 & -\sigma^3 \end{pmatrix}, \quad \Gamma^t = \begin{pmatrix} i\sigma^1 & 0 \\ 0 & i\sigma^1 \end{pmatrix}, \quad \Gamma^1 = \begin{pmatrix} -\sigma^2 & 0 \\ 0 & \sigma^2 \end{pmatrix}, \quad \Gamma^2 = \begin{pmatrix} 0 & -i\sigma^2 \\ i\sigma^2 & 0 \end{pmatrix}. \quad (6)$$

The Dirac equation can be rewritten into

$$\sqrt{g^{rr}}\partial_r \begin{pmatrix} F_1 \\ F_2 \end{pmatrix} + m\sigma^3 \otimes \begin{pmatrix} F_1 \\ F_2 \end{pmatrix} = \sqrt{g^{tt}}(\omega + qA_t)i\sigma^2 \otimes \begin{pmatrix} F_1 \\ F_2 \end{pmatrix} \mp k\sqrt{g^{xx}}\sigma^1 \otimes \begin{pmatrix} F_1 \\ F_2 \end{pmatrix} - p\sqrt{g^{tt}g^{rr}}\partial_r A_t \sigma^1 \otimes \begin{pmatrix} F_1 \\ F_2 \end{pmatrix}. \quad (7)$$

Furthermore, to decouple the equation of motion, we take the decomposition $F_\pm = \frac{1}{2}(1 \pm \Gamma^r)F$ with

$$F_+ = \begin{pmatrix} 0 \\ \mathcal{B}_1 \\ 0 \\ \mathcal{B}_2 \end{pmatrix}, \quad F_- = \begin{pmatrix} \mathcal{A}_1 \\ 0 \\ \mathcal{A}_2 \\ 0 \end{pmatrix}, \quad \text{and} \quad F_\alpha \equiv \begin{pmatrix} \mathcal{A}_\alpha \\ \mathcal{B}_\alpha \end{pmatrix}, \quad \alpha = 1, 2. \quad (8)$$

Under such decomposition, the Dirac equation (7) can be divided into

$$(\sqrt{g^{rr}}\partial_r \pm m) \begin{pmatrix} \mathcal{A}_1 \\ \mathcal{B}_1 \end{pmatrix} = \pm(\omega + qA_t)\sqrt{g^{tt}} \begin{pmatrix} \mathcal{B}_1 \\ \mathcal{A}_1 \end{pmatrix} - (k\sqrt{g^{xx}} + p\sqrt{g^{tt}g^{rr}}\partial_r A_t) \begin{pmatrix} \mathcal{B}_1 \\ \mathcal{A}_1 \end{pmatrix}, \quad (9)$$

$$(\sqrt{g^{rr}}\partial_r \pm m) \begin{pmatrix} \mathcal{A}_2 \\ \mathcal{B}_2 \end{pmatrix} = \pm(\omega + qA_t)\sqrt{g^{tt}} \begin{pmatrix} \mathcal{B}_2 \\ \mathcal{A}_2 \end{pmatrix} + (k\sqrt{g^{xx}} - p\sqrt{g^{tt}g^{rr}}\partial_r A_t) \begin{pmatrix} \mathcal{B}_2 \\ \mathcal{A}_2 \end{pmatrix}. \quad (10)$$

It is straightforward to reduce the above two equations into the flow equation of $\xi_I \equiv \frac{A_I}{B_I} (I = 1, 2)$

$$(\sqrt{f}e^B\partial_r + 2m)\xi_I = [v_- + (-1)^I e^{-B}k] + [v_+ - (-1)^I k e^{-B}] \xi_I^2 \quad (11)$$

where $v_{\pm} = \frac{e^{-B}}{\sqrt{f}} [\omega + qA_t] \pm pA_t'$.

Near the AdS boundary, from (7) we see that the reduced Dirac field behaves as

$$F_I \stackrel{r \rightarrow \infty}{\approx} a_I r^{-mL} \begin{pmatrix} 1 \\ 0 \end{pmatrix} + b_I r^{mL} \begin{pmatrix} 0 \\ 1 \end{pmatrix}, \quad I = 1, 2. \quad (12)$$

Then the value $G_I = \frac{a_I}{b_I}$ can be expressed in the form

$$G_I = \lim_{r \rightarrow \infty} r^{2m} \xi_I \quad (13)$$

Thus, we can read off G_I by solving the flow equation (11) with the boundary condition at the horizon[10]

$$\xi_I = \begin{cases} i & \text{for } \omega \neq 0; \\ (-1)^I \text{sign}(k) & \text{for } \omega = 0. \end{cases} \quad (14)$$

It is worth indicating that from the flow equation (11) and the above boundary condition, we can find G_I with the following symmetries:

$$\begin{aligned} G_1(\omega, k) &= G_2(\omega, -k); \\ G_1(\omega, k; q, p) &= -G_2^*(-\omega, k; -q, -p). \end{aligned} \quad (15)$$

Especially, when $m = 0$, G_1 and G_2 satisfy the relation

$$G_1(\omega, k) = -\frac{1}{G_2(\omega, k)}. \quad (16)$$

B. Non-relativistic fermionic fixed point

Most available works on the holographic fermionic systems focus on the perturbations on the relativistic fixed point by keeping the Lorentz invariance for the boundary theory. In [7], the authors first considered the boundary term by dropping the Lorentz invariance while still keeping the $U(1)$ global symmetry $\psi \rightarrow e^{i\theta}\psi$, the rotational invariance as well as the scale invariance. In this spirit, the boundary term to the bulk action (1) reads

$$S_{bdy} = \frac{1}{2} \int_{\partial\mathcal{M}} d^3x \sqrt{-g g^{rr}} \bar{\zeta} \Gamma^1 \Gamma^2 \zeta. \quad (17)$$

This boundary term keeps the variational principle well-defined.

The variation of the on-shell action for the Dirac spinor has the form

$$\delta S_D = \delta S_{bulk} + \delta S_{bdy} = - \int d^3x (\delta B_+^\dagger A_+ + B_-^\dagger \delta A_- + A_+^\dagger \delta B_+ + \delta A_-^\dagger B_-) \quad (18)$$

with $(A_+, A_-) = \frac{1}{\sqrt{2}}(\mathcal{A}_1 + \mathcal{A}_2, \mathcal{A}_1 - \mathcal{A}_2)$ and $(B_+, B_-) = \frac{1}{\sqrt{2}}(\mathcal{B}_1 + \mathcal{B}_2, \mathcal{B}_2 - \mathcal{B}_1)$.

We can extract two groups of fermionic source and the dual operator, which are (B_+, A_+) and (A_-, B_-) . The dimension of the operators are $\frac{3}{2} + m$ and $\frac{3}{2} - m$, respectively [7].

According to the AdS/CFT dictionary, the retarded Green function for the non-relativistic fermionic fixed point can be defined as

$$\begin{pmatrix} A_+ \\ B_- \end{pmatrix} = G_R \begin{pmatrix} B_+ \\ A_- \end{pmatrix}. \quad (19)$$

Following the analysis in [10], the matrix $G_R = \begin{pmatrix} \frac{2G_1G_2}{G_1+G_2} & \frac{G_1-G_2}{G_1+G_2} \\ \frac{G_1-G_2}{G_1+G_2} & \frac{2G_1G_2}{G_1+G_2} \end{pmatrix}$ is off-diagonal and its eigenvalue λ_\pm can be expressed in terms of G_I as

$$\lambda_\pm = \frac{G_1G_2 - 1 \pm \sqrt{1 + G_1^2 + G_2^2 + G_1^2G_2^2}}{G_1 + G_2}. \quad (20)$$

Thus, the spectral function has the form

$$A(\omega, k) = Tr[Im G_R] = \frac{2G_1G_2 - 2}{G_1 + G_2}. \quad (21)$$

III. NUMERICAL RESULTS

We numerically integrate the flow equation (11) and read off the asymptotic values to compute the retarded Green functions with the Lorentz violating boundary term in the charged dilatonic AdS black hole background. We will calculate the fermion spectral function and also the density of states. We will investigate the effects of the dipole coupling and the dilaton field on the holographic fermionic system.

A. Zero temperature

In this subsection, we will show our numerical results of the massless fermion in the limit of zero temperature. For convenience, we fix $L = 1$. The chemical potential reads $\mu = -\sqrt{3}Q$.

1. The dipole effect on the flat band and the Fermi surface

We choose $Q = 1$ in this subsection. In our computation we first set $q = 1$. The numerical results for the spectral function are shown in Figs.1-4.

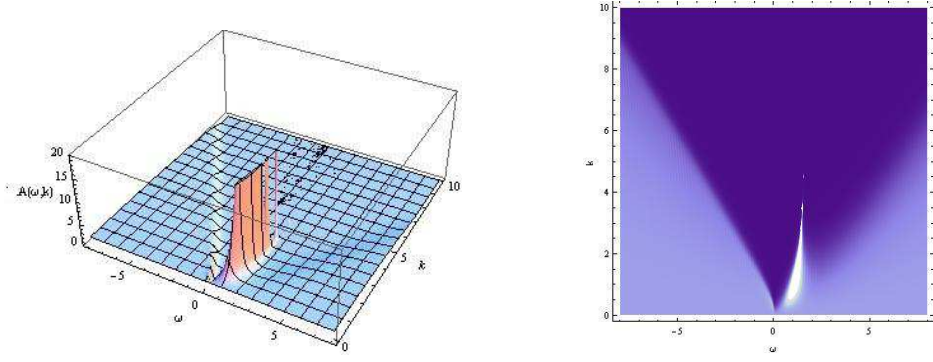


FIG. 1: The plots of $A(\omega, k)$ for the case of $q = 1$ and $p = 0$.

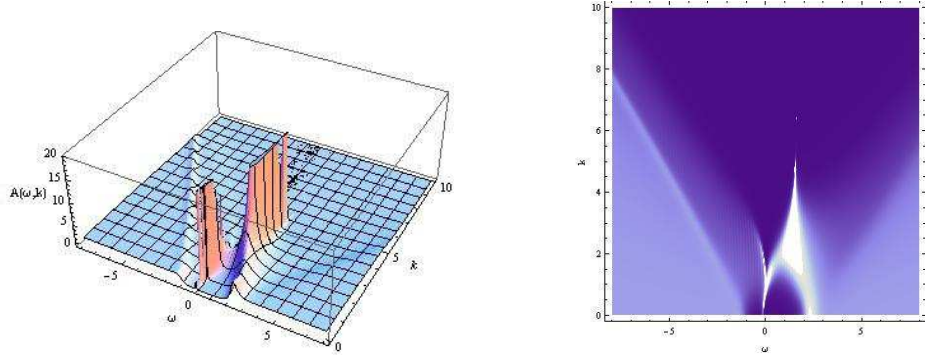


FIG. 2: The plots of $A(\omega, k)$ for the case of $q = 1$ and $p = 2$.

When there is no dipole coupling between the fermionic field and the gauge field, $p = 0$, the result shown in Fig.1 goes back to figure 1 in [10] for the non-relativistic fixed point. Clearly, we see that $A(\omega, k)$ shows the flat band with the peculiar property of poles distributing continuously at a finite interval of momenta. This finite band is mildly dispersed at low momentum, but it presents strong peak at high momentum. This is because that the high momentum modes sit outside the lightcone and can't decay. The peak tends sharper as can be checked by plotting a suitable cross section at fixed high k .

We now turn on the dipole coupling parameter p and report the results in Figs.2-4. At low momentum, the flat band gets more dispersed and the band recovers flatness at higher momentum when the non-minimum fermion coupling becomes stronger. With the increase of the dipole coupling, the frequency of the flat band is larger and the peak of the flat band becomes sharper at small momenta, which means that more energy is needed to excite the small momentum modes for larger p . A finite gap opens up and enlarges when the dipole coupling becomes strong. The further extreme behavior of the flat band shows the physics approaching a more strongly coupled corner when the dipole coupling becomes stronger. Furthermore we observe that at large enough momentum the flat band always shifts to $\omega = \sqrt{3}$ for all dipole coupling. This property can be attributed to the frequency ω which is measured relative to the chemical potential.

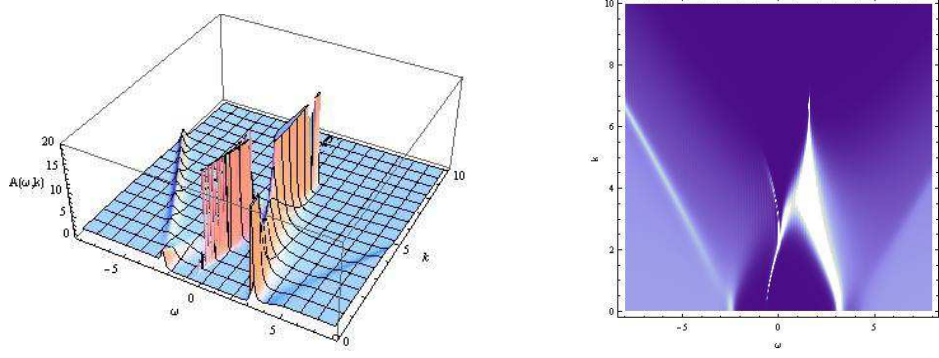


FIG. 3: The plots of $A(\omega, k)$ for the case of $q = 1$ and $p = 4$.

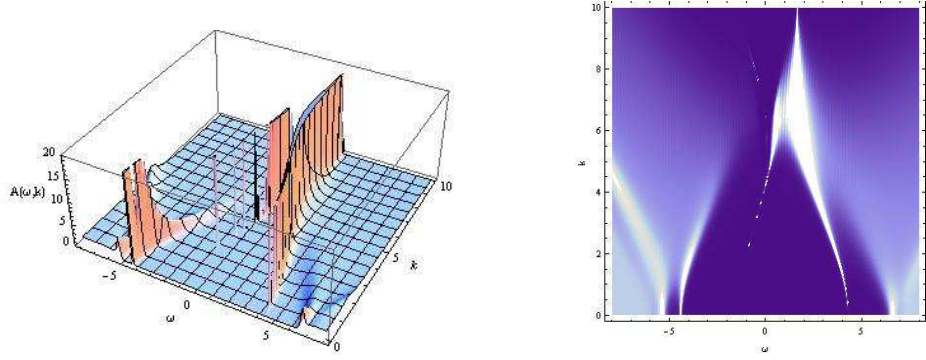


FIG. 4: The plots of $A(\omega, k)$ for the case of $q = 1$ and $p = 8$.

The appearance of the flat band for the non-relativistic fermions observed here is interesting, which has not been observed for the relativistic fermions in the charged dilatonic AdS black hole background [22]. The different properties between the non-relativistic and relativistic fermions observed here support the findings in [9] by comparing with [19] for the charged AdS black hole background.

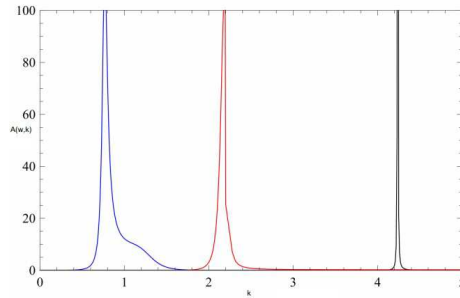


FIG. 5: The function of $A(\omega, k)$ at $\omega = -10^{-7}$ for different dipole coupling. The lines from left to right are for $p = 2, 4$ and 8 , respectively. In the computation we take $q = 1$.

Now we turn to discuss the fermi momentum. From Fig.1-4 we see that the Fermi surface opens up for nonzero p . In the limit $\omega \rightarrow 0$, the sharp peak of the spectral function represents the fermi surface. For various values of p we illustrate the location of Fermi surface in Fig.5. We find that the corresponding

p	0	2	4	8
k_F	No	0.76806283	2.19010221	4.23765084
v_F	No	0.286127	0.444296	0.401080

TABLE I: The Fermi momentum and Fermi velocity for different dipole couplings when we choose $q = 1$.

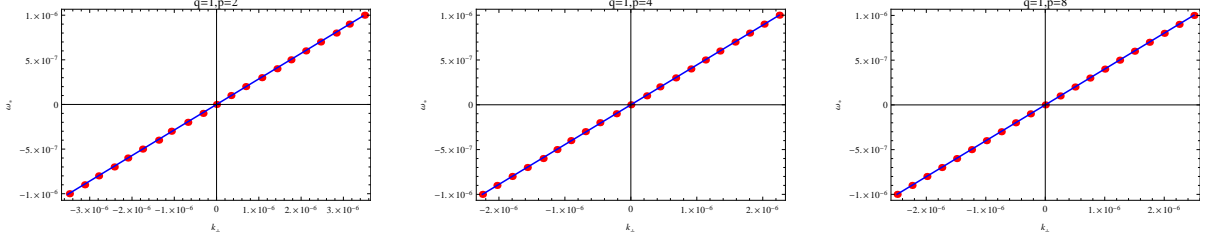


FIG. 6: The dispersion relation near the Fermi surface at the Non-relativistic fixed point of $q = 1$ for various p .

Fermi momentum increases when the dipole interaction becomes stronger as shown in Table.I. We can further investigate the dispersion relation near the Fermi surface. For various p we show in Fig.6 that the linear relation between ω and $k_{\perp} = k - k_F$ behaves as

$$\omega \simeq v_F k_{\perp}. \quad (22)$$

This linear dispersion relation indicates that the excitation near the Fermi surface is well-defined and the Fermi liquid is like the Landau Fermi liquid. This property is not influenced by the dipole coupling, which is consistent with the case of relativistic fermions discussed in [22]. The values of the Fermi velocity $v_F = \frac{\partial \omega}{\partial k}$ for different dipole coupling are listed in Table.I.

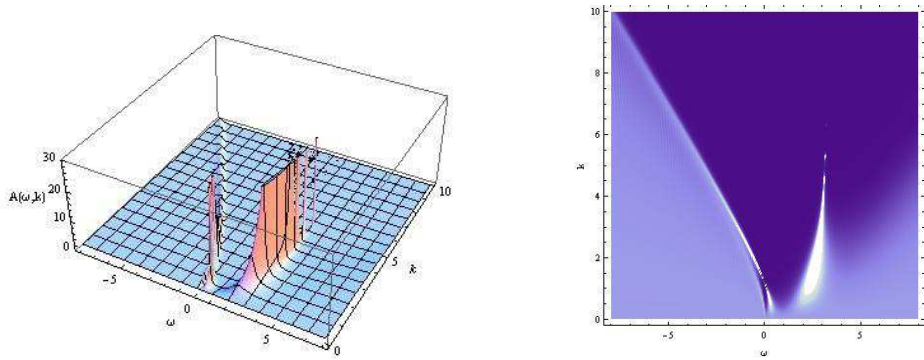
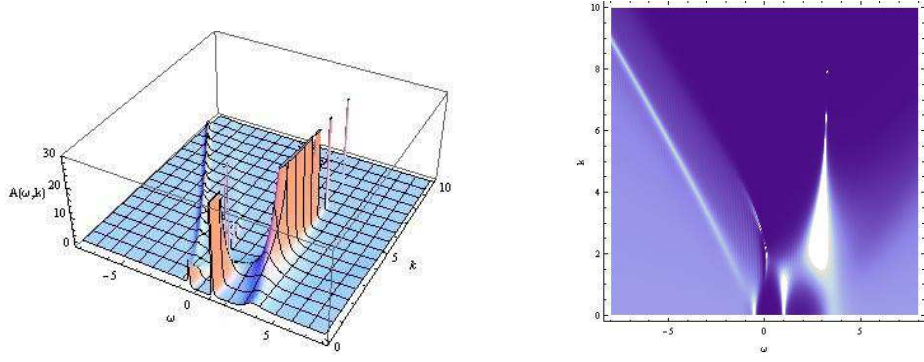
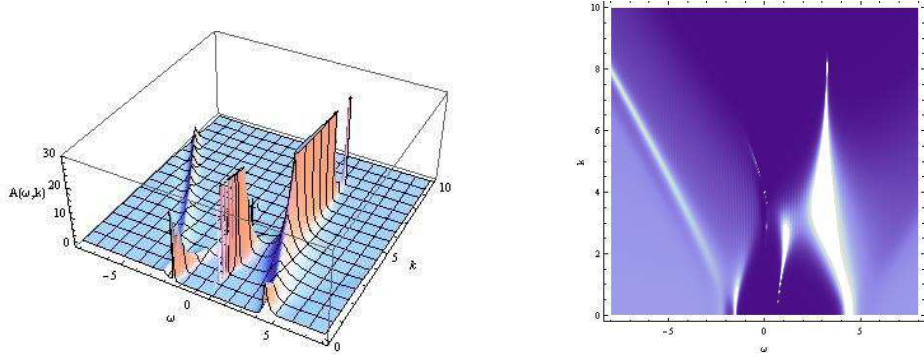


FIG. 7: The plots of $A(\omega, k)$ for the case of $q = 2$ and $p = 0$.

We will also discuss the influence of the q value on the fermion system. In [26], it was claimed that the charge q can affect the excitation near the Fermi surface. In addition, it was argued that there is some kind of competition between the charge q and the dipole coupling p to create the Fermi surface for the non-relativistic fixed point in charged AdS black hole [10]. Here we would like to further examine the effect of q in the Fermi system in the charged dilatonic AdS background. We will change the value of q in the computation and

FIG. 8: The plots of $A(\omega, k)$ for the case of $q = 2$ and $p = 2$.FIG. 9: The plots of $A(\omega, k)$ for the case of $q = 2$ and $p = 4$.

compare with the result for $q = 1$. The spectral functions are shown in Fig.7-10 for taking $q = 2$. Similar to the results by setting $q = 1$, flat bands tend to $2\sqrt{3}$ at large enough momentum which is independent of the dipole coupling. Besides the similarity, we observe the different property for choosing different q . When $q = 2$, we see that the quasi-particle like peak, i.e., Fermi surface appears even at $p = 0$. This is different from small q case where there is no Fermi surface in the $\omega = 0$ limit for the minimal Fermion coupling. Moreover, the emergence of the gap can happen at smaller dipole coupling when q is big, for example the gap emerges around $p \sim 13$ for $q = 1$, while the gap appears around $p \sim 8.5$ when $q = 2$. These observations support that q value is nontrivial, it influences the Fermi system.

The Fermi momentum and Fermi velocity for choosing $q = 2$ are listed in Table.II. Similar to setting $q = 1$, the Fermi momentum increases with p and the dispersion relation is kept linear, independent of the change q [10]. Comparing with the relativistic situation [22], we find that for the same bulk coupling, the

p	0	2	4	8
k_F	1.18628543	2.33984327	3.99854464	7.40908575
v_F	-0.607729	-0.380546	-0.380714	-0.382852

TABLE II: The Fermi momentum and Fermi velocity for different dipole couplings for $q = 2$.

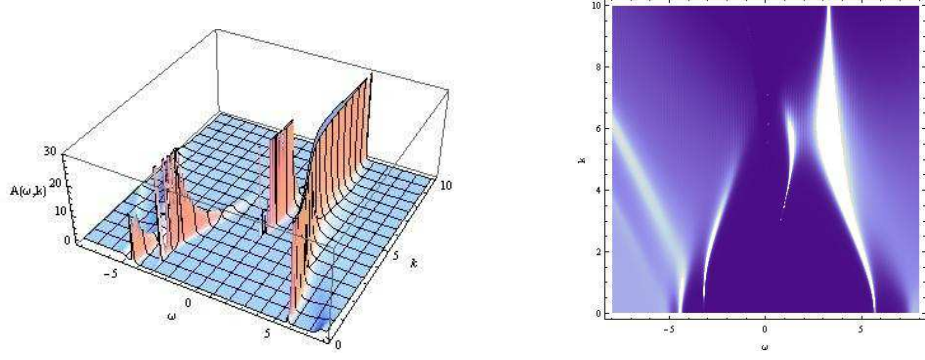


FIG. 10: The plots of $A(\omega, k)$ for the case of $q = 2$ and $p = 8$.

Fermi momentum is smaller in the non-relativistic case. The suppression of the Fermi momentum in the non-relativistic case can attribute to the presence of the flat band. In addition, we find that the Fermi velocities for $q = 2$ and $q = 1$ have opposite signs. These imply that the charge q do influence the excitation near the Fermi surface which supports the claim in [26].

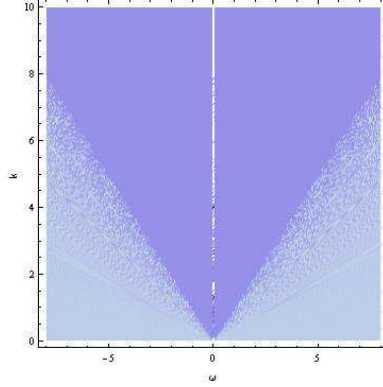


FIG. 11: $A(\omega, k)$ with $q = p = 2$ for $Q = 0$.

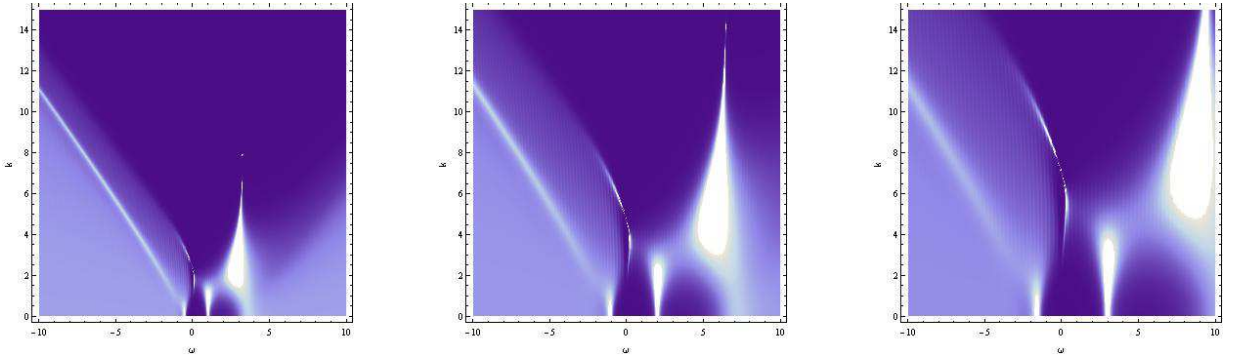
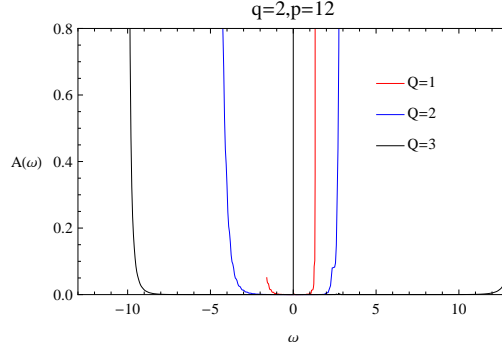


FIG. 12: The plots of $A(\omega, k)$ with $q = p = 2$. Here Q is set to be 1, 2 and 3 respectively from left to right.

Q	0	1	2	3
k_F	No	2.33984327	4.67974416	7.01962931

TABLE III: The Fermi momentum for different Q with $q = p = 2$.FIG. 13: $A(\omega)$ for different values of Q at zero temperature.

2. The influence of the dilaton field

We now investigate how the dilaton field influence the behavior of the spectral function. Without loss of generality, we set $q = p = 2$ in the discussion. When the dilaton field vanishes $Q = 0$, the background (2) goes back to the AdS Schwarzschild black hole. The spectral function for $Q = 0$ is shown in Fig.11. This background is not charged, so that it does not have Fermi-like peak.

In the dilaton gravity, the chemical potential is finite as described in (4). This gives the possibility of fermionic excitation. The numerical results on the spectral function for nonzero values of Q are shown in Fig.12. We observe the Fermi-like peak and present the Fermi momentum in Table.III. The Fermi momentum increases but the peak becomes lower as the increase of the dilaton field Q . For larger Q , the flat band gets more dispersed in the low momentum and the peak of the band appears at higher momentum. This shows that the dilaton field has the effect on the shift of the flat band.

To see clearly the effect of the dilaton field on the gap, we plot the density of state by integrating $A(\omega, k)$ over k with strong dipole coupling $p = 12$ in Fig.13. We observe that with the increase of Q , the gap becomes wider. This tells us that in the dilaton gravity the effect of the dipole coupling will be more explicit.

B. Finite temperature

In [20][22], it was argued that the gap brought by strong dipole coupling will vanish once the temperature increases to a critical value for the relativistic fermionic system. It is of interest to examine this property for the non-relativistic situation by imposing Lorentz breaking boundary conditions.

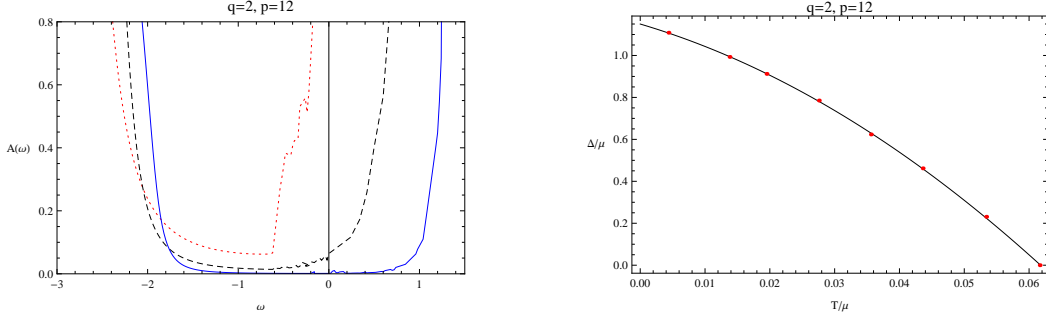


FIG. 14: Left: $A(\omega)$ as a function of ω when $Q = 1$ at finite temperatures. T/μ are 0.0435864(solid), 0.0616404(dashed) and 0.0754938(dotted). Right: The width of the gap as a function of the temperature.

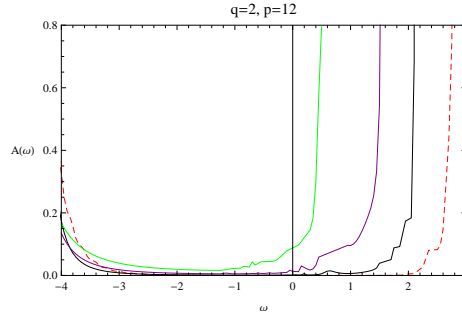


FIG. 15: $A(\omega)$ as a function of ω when $Q = 2$ at finite temperatures. T/μ are 0(red dashed), 0.0435864(black), 0.0533822(purple) and 0.0616404(green), respectively.

We calculate the spectral function at the finite temperature. We set $q = 2$ and $p = 12$ in the following discussion. In the left panel of Fig.14, we show the density of state for different temperatures when the dilaton $Q = 1$. We see that the gap becomes narrower and closes up when T/μ increases to the value 0.061. Moreover, we show the width of the gap Δ as a function of T in the right panel of Fig.14. As the temperature increases to T_* when the gap closes up, there is a transition from the insulator to conducting state. In our model, We find the ratio Δ_*/T_* is around 18.65, where Δ_* is the width of the gap at zero temperature. This supports that the generated gap is temperature-dependent. Our value of Δ_*/T_* is approximately close to 20 in vanadium dioxide[27]. In the charged AdS black hole background, the ratio Δ_*/T_* was found around 10 [20].

We also calculate the spectral function for different dilaton charge, for example taking $Q = 2$. The density of state for different temperature is shown in Fig.15. The property that gap becoming narrower for higher temperature holds as well. For bigger dilaton charge, we find that the value of Δ_*/T_* is higher, where T_* is the temperature to close up the gap. When $Q = 2$, the value of Δ_*/T_* is around 27.82. It is worth noting that similar to the case of zero temperature, the gap becomes wider as we increase Q for fixed finite temperature, this is explicit by comparing Fig.14 and Fig.15.

IV. DISCUSSION AND CONCLUSION

We have studied extensively the properties of the holographic non-relativistic fermionic fixed points in the charged dilatonic black hole background. We have disclosed the influence on the relevant spectral function by the dipole coupling between the fermion and gauge field in the bulk. We showed that there always exists a flat band which tends to a finite value at large momenta limit for the nonrelativistic fermi system. For the stronger dipole coupling, we observed that the value of the momenta for the peak of flat band is larger and the peak of the band at low momenta becomes sharper. The Fermi momentum increases as the dipole coupling becomes stronger, while the linear dispersion relation is still kept which is independent of the dipole coupling and the charge. When p is close to a critical value, a gap opens up and becomes wider as we further increase the coupling. This critical value depends on the charge, which is smaller for bigger q . We also discussed how the dilaton field influence the dipole effect. Further we found that the width of the gap is temperature-dependent.

The properties for the nonrelativistic fermion system disclosed here in the holographic study with the modification of the boundary term are interesting. The disclosed coincidence of the holographic ratio between the width of the gap at zero temperature and the temperature for the gap vanishing with the value in the vanadium dioxide [27] is encouraging, although the deep understanding is still lacking. It is of interest to further explore the holographic properties of the nonrelativistic fermion system and it is expected that the theoretical attempt can help to unlock more puzzles in the condense matter physics. Further investigations on this topic are called for.

Acknowledgments

This work was supported partially by the NNSF of China and the Shanghai Science and Technology Commission under the grant 11DZ2260700.

-
- [1] S.A. Hartnoll, *Class. Quant. Grav.* **26**, 224002 (2009), [arXiv:0903.3246].
 - [2] C.P. Herzog, *J. Phys. A* **42**, 343001 (2009), [arXiv:0904.1975].
 - [3] G.T. Horowitz, [arXiv: 1002.1722].
 - [4] S. S. Gubser, F. D. Rocha, *Phys. Rev. D* **81**, 046001 (2010), [arXiv:0911.2898];
 - [5] K. Goldstein, S. Kachru, S. Prakash and S. P. Trivedi, *JHEP* **1008** (2010) 078, [arXiv:1007.2490].
 - [6] C. Charmousis, B. Gouteraux, B. S. Kim, E. Kiritsis and R. Meyer, *JHEP* **1011** (2010) 151. [arXiv:1005.4690].
 - [7] J. N. Laia, D. Tong, *JHEP* **1111** (2011) 125, [arXiv:1108.1381].
 - [8] J. N. Laia, D. Tong, *JHEP* **1111** (2011) 131 [arXiv:1108.2216]
 - [9] W. J. Li, H. Zhang, *JHEP* **1111**(2011) 018, [arXiv:1110.4559].
 - [10] W. J. Li, R. Meyer, H. Zhang, *JHEP* **1201** (2012) 153, [arXiv:1111.3783].
 - [11] W. J. Li, J. P. Wu, [arXiv:1203.0674]
 - [12] S. S. Lee, *Phys. Rev. D* **79**, 086006, (2009), [arXiv:0809.3402].

- [13] N. Iqbal and H. Liu, Phys. Rev. D 79, 025023 (2009), [arXiv:0809.3808].
- [14] H. Liu, J. McGreevy and D. Vegh, Phys. Rev. D 83, 065029 (2011), [arXiv:0903.2477].
- [15] N. Iqbal and H. Liu, Fortsch. Phys. 57, 367 (2009), [arXiv:0903.2596].
- [16] M. Cubrovic, J. Zaanen and K. Schalm, Science 325 (2009) 439, [arXiv:0904.1993].
- [17] J. P. Wu, JHEP 1107:106,2011, [arXiv:1103.3982].
- [18] L. Q. Fang, X. H. Ge, X. M. Kuang, [arXiv:1201.3832].
- [19] M. Edalati, R. G. Leigh, P. W. Phillips, Phys. Rev. Lett. 106, 091602 (2011), [arXiv:1010.3238].
- [20] M. Edalati, R. G. Leigh, K. W. Lo, P. W. Phillips, Phys. Rev. D 83, 046012 (2011), [arXiv:1012.3751].
- [21] J. P. Wu, H. B. Zeng, JHEP 1204 (2012) 068, [arXiv:1201.2485].
- [22] W. Y. Wen, S. Y. Wu, Phys.Lett. B712 (2012) 266-271, [arXiv:1202.6539].
- [23] X. M. Kuang, B. Wang, J. P. Wu, JHEP 07 (2012) 125, [arXiv:1205.6674].
- [24] R. M. Wald, "General Relativity", The University of Chicago Press.
- [25] T. Faulkner, G. T. Horowitz, J. McGreevy, M. M. Roberts, D. Vegh, JHEP 1003, 121 (2010), [arXiv:0911.3402].
- [26] S. S. Gubser, Jie Ren, Phys.Rev.D86:046004,2012,[arXiv:1204.6315]
- [27] A. Zylbersztejn and N. F. Mott, Phys. Rev. B11, 4383 (1975).